Robust STAP Detection Based on Volume Cross-Correlation Function in Heterogeneous Environments

Zhizhuo Jiang, You He, Gang Li, *Senior Member, IEEE*, and Xiao-Ping Zhang, *Senior Member, IEEE*

***Abstract*— The performance of moving target detection in heterogeneous environments with the traditional space-time adaptive processing (STAP) may degrade when the real clutter environments deviate from the prior assumption on the clutter distribution. In this letter, a new detector for STAP applications based on volume cross-correlation function (VCF), namely VCF-STAP, is proposed to achieve robust performance of moving target detection in heterogeneous environments. In the new VCF-STAP, the VCF is used to form a distance measure between the sample signal subspace and the target subspace without modeling the clutter distribution. Then, a new robust STAP detection statistic is constructed using this distance measure. Simulation and experimental results show that the proposed VCF-STAP achieves robust performance of moving target detection in heterogeneous environments, especially it achieves much superior detection performance compared with existing STAP methods when the real clutter environments do not satisfy their prior assumptions. Besides, it is also shown that VCF-STAP has the constant false alarm rate (CFAR) property.**

***Index Terms*— Heterogeneous environments, moving target detection, space-time adaptive processing (STAP), volume cross-correlation function (VCF).**

I. Introduction

MOVING target detection with space-time adaptive processing (STAP) in heterogeneous environments is an intractable problem and has received extensive attention [1]–[3]. In STAP techniques, it is required to estimate the clutter covariance matrix (CCM) using independent and identically distributed (IID) training samples and then suppress the clutter.

However, it is often difficult to obtain enough IID training samples in heterogeneous environments [4]. As such, the target detection performances with traditional STAP methods degrade in heterogeneous environments. To enhance the detection performance with STAP in heterogeneous environments, several parametric distribution-based methods of estimation of the CCM are proposed [5], [6] with limited training samples. In [5], a maximum *a posteriori* (MAP) estimation of the CCM in the cell under test (CUT) is derived based on the assumption that the CCM in the CUT satisfies the complex Wishart distribution when the CCMs in the training samples are given. In [6], under the assumption of the invert Wishart distribution for the CCMs in the training samples, the authors develop a maximum likelihood estimation of the CCM in the CUT. However, the detection performances of distribution-based methods significantly deteriorate when the real clutter environments deviate from their prior assumption on the clutter distribution.

In this letter, we propose a new detector based on volume cross-correlation function (VCF) for the STAP applications, referred to as VCF-STAP, to achieve robust performance of moving target detection in heterogeneous environments. In the new VCF-STAP, the training samples are employed to span the sample signal subspace. The VCF is utilized to form a distance measure between the sample signal subspace and the target subspace. Then, a new robust STAP detection statistic is formulated as the difference value of the reciprocal of VCF values. Moreover, a correction strategy is proposed to eliminate the impact of the target energy leakage. Different from existing distribution-based methods, VCF-STAP does not need CCM estimation and clutter suppression. It implements detection directly by measuring the distance between the target subspace and the sample signal subspace, without any prior assumption on the clutter distribution. Thus, it is more robust than existing distribution-based STAP methods in heterogeneous environments. The superiority of VCF-STAP is verified by both simulated data and measured Mountain-Top data.

II. Problem Formulation

Consider an airborne radar with N array elements where M pulses are received in a coherent processing interval (CPI). The detection problem for STAP applications is considered as the conventional binary composite hypothesis testing problem [5]

$$H_0 : \begin{cases} \boldsymbol{x} = \boldsymbol{c}; \\ \boldsymbol{x}_q = \boldsymbol{c}_q; q = 1, \dots, Q \end{cases}$$
$$H_1 : \begin{cases} \boldsymbol{x} = \alpha \boldsymbol{s} + \boldsymbol{c}; \\ \boldsymbol{x}_q = \boldsymbol{c}_q; q = 1, \dots, Q \end{cases} \tag{1}$$

where $\boldsymbol{x} \in \mathbb{C}^{NM\times 1}$ is the space-time data in the CUT, $\boldsymbol{x}_q \in \mathbb{C}^{NM\times 1}, q = 1, \dots, Q$ denote the qth training sample, and q and Q are the range cell index and the number of training samples, respectively. The spatial-temporal steering vector of the target is denoted as $\boldsymbol{s} \in \mathbb{C}^{NM\times 1}$ with a complex

Manuscript received April 11, 2020; revised July 21, 2020; accepted August 17, 2020. Date of publication September 9, 2020; date of current version December 31, 2021. This work was supported in part by the National Natural Science Foundation of China under Grant 61790551 and Grant 61925106. *(Corresponding author: You He.)*

Zhizhuo Jiang and Gang Li are with the Department of Electronic Engineering, Tsinghua University, Beijing 100084, China.

You He is with the Institute of Information Fusion, Naval Aviation University, Yantai 264001, China, also with the Department of Electronic Engineering, Tsinghua University, Beijing 100084, China (e-mail: heyou_f@126.com).

Xiao-Ping Zhang is with the Department of Electrical, Computer and Biomedical Engineering, Ryerson University, Toronto, ON M5B 2K3, Canada.

Digital Object Identifier 10.1109/LGRS.2020.3019580

amplitude α. The notations $\boldsymbol{c} \in \mathbb{C}^{NM\times 1}$ and $\boldsymbol{c}_q \in \mathbb{C}^{NM\times 1}$ stand for clutter plus noise returns in the CUT and that in the training data, which are complex Gaussian distributed with zero mean and covariance matrices $\boldsymbol{R}_u$ and $\boldsymbol{R}_\upsilon$, respectively, where the subscript u and υ indicate the CUT and the training data, namely

$$\begin{aligned} \boldsymbol{c} &\sim \mathcal{CN}(\boldsymbol{0}, \boldsymbol{R}_u) \\ \boldsymbol{c}_q &\sim \mathcal{CN}(\boldsymbol{0}, \boldsymbol{R}_\upsilon). \end{aligned} \tag{2}$$

In practice, $\boldsymbol{R}_u$ is always unknown and need to be estimated. In traditional distribution-based methods, the distribution of $\boldsymbol{R}_u$ or $\boldsymbol{R}_\upsilon$ is required to estimate $\boldsymbol{R}_u$ and then the target detection is accomplished after the clutter is suppressed [5], [6].

III. VCF-Based Detector for STAP

In this section, the new VCF-STAP is proposed. Specifically, training samples are utilized to span the sample signal subspace, then the VCF is employed to form the distance measure between the sample signal subspace and the target subspace. Finally, the new robust STAP detection statistic is formulated.

A. Estimation of the Sample Signal Subspace

We use $\mathcal{P}_s$ and $\mathcal{P}_t$ to denote the sample signal subspace and the target subspace, respectively, and the subscript s and t indicate the sample signal and the target, respectively. Specifically, the sample signal subspace is spanned by the observed radar signal, and the target subspace is spanned by the target signals. Let K and L represent the dimension of $\mathcal{P}_s$ and $\mathcal{P}_t$, respectively. Note that in VCF-STAP, the training samples do not need to be IID and, therefore, the number of training samples is sufficient.

For each range cell, a fixed-length window is employed to the received radar signal to form the training sample matrix, and the detection is implemented by sliding the window along the range axis. Specifically, the training sample matrix $\boldsymbol{X}(q) = \left[\boldsymbol{x}_{q-Q+1}, \boldsymbol{x}_{q-Q+2}, \ldots, \boldsymbol{x}_q\right] \in \mathbb{C}^{NM\times Q}$ is selected by utilizing the window of length Q for the qth range cell. Then, the corresponding covariance matrix $\boldsymbol{R}(q)$ is obtained

$$\boldsymbol{R}(q) = \boldsymbol{X}(q)\boldsymbol{X}(q)^H/Q \tag{3}$$

where $(\cdot)^H$ is the operator of conjugate transpose. To reduce the effect of noise subspace and obtain the basis matrix corresponding to the sample signal subspace, we perform eigenvalue decomposition on $\boldsymbol{R}(q)$. The eigenvalues of $\boldsymbol{R}(q)$ are denoted as $\lambda_1, \lambda_2, \ldots, \lambda_{NM}$, where

$$\lambda_1 \geq \lambda_2 \geq \cdots \geq \lambda_K \geq \lambda_{K+1} = \cdots = \lambda_{NM} \tag{4}$$

and the corresponding eigenvectors are $\boldsymbol{t}_1, \boldsymbol{t}_2, \ldots, \boldsymbol{t}_K, \boldsymbol{t}_{K+1}, \ldots, \boldsymbol{t}_{NM}$. The estimated basis matrix $\hat{\boldsymbol{T}}_s(q) \in \mathbb{C}^{NM\times K}$ of the sample signal subspace is formed by K dominant eigenvectors, that is

$$\hat{\boldsymbol{T}}_s(q) = [\boldsymbol{t}_1, \boldsymbol{t}_2, \ldots, \boldsymbol{t}_K]. \tag{5}$$

For the target subspace $\mathcal{P}_t$, the corresponding basis matrix $\boldsymbol{T}_t \in \mathbb{C}^{NM\times L}$ is estimated by the Gram–Schmidt orthogonalization of the spatial-temporal steering vector(s) of the target(s) [7], i.e., the target subspace is determined by the spatial-temporal steering vector(s) of the target(s).

B. New VCF-Based STAP Detection Statistic

By introducing the principal angle between two subspaces, it has been proven in [8] that the VCF provides a metric of the distance between the sample signal subspace $\mathcal{P}_s$ and the target subspace $\mathcal{P}_t$, defined by

$$\mathrm{VCF}\left(\hat{\boldsymbol{T}}_s(q), \hat{\boldsymbol{T}}_t\right) = \frac{\mathrm{vol}_{K+L}\left(\left[\hat{\boldsymbol{T}}_s(q), \hat{\boldsymbol{T}}_t\right]\right)}{\mathrm{vol}_K\left(\hat{\boldsymbol{T}}_s(q)\right)\mathrm{vol}_L\left(\hat{\boldsymbol{T}}_t\right)} \tag{6}$$

where $[\cdot,\cdot]$ is the concatenating operator of two matrices along the column dimension, and $\hat{\boldsymbol{T}}_t$ is the estimated basis matrix of the target subspace. Take $\hat{\boldsymbol{T}}_s(q)$ as an example, the geometrical volume of K-dimensional parallelotope spanned by $\hat{\boldsymbol{T}}_s(q)$ is measured by $\mathrm{vol}_K\left(\hat{\boldsymbol{T}}_s(q)\right)$ [9], defined by

$$\mathrm{vol}_K\left(\hat{\boldsymbol{T}}_s(q)\right) = \prod_{i=1}^{K} \delta_i \tag{7}$$

where $\delta_1, \delta_2, \ldots, \delta_K \geq 0$ are the singular values of $\hat{\boldsymbol{T}}_s(q)$.

Because $\hat{\boldsymbol{T}}_s(q)$ and $\hat{\boldsymbol{T}}_t$ are orthonormal bases, the distance measure in (6) is derived as [7]

$$\mathrm{VCF}\left(\hat{\boldsymbol{T}}_s(q), \hat{\boldsymbol{T}}_t\right) = \mathrm{vol}_{K+L}\left(\left[\hat{\boldsymbol{T}}_s(q), \hat{\boldsymbol{T}}_t\right]\right) \tag{8}$$

by substituting $\mathrm{vol}_K(\hat{\boldsymbol{T}}_s(q)) = \mathrm{vol}_L(\hat{\boldsymbol{T}}_t) = 1$.

Theoretically, $\mathrm{VCF}(\hat{\boldsymbol{T}}_s(q), \hat{\boldsymbol{T}}_t)$ tends to be a small value when $\mathcal{P}_s$ and $\mathcal{P}_t$ intersect; otherwise, it tends to be large [8].

Note that the columns of the basis matrices of $\mathcal{P}_s$ and $\mathcal{P}_t$ are normalized. Accordingly, the distance measure between $\mathcal{P}_s$ and $\mathcal{P}_t$ in (8) is independent of the clutter power. Therefore, the threshold is independent of the clutter-to-noise-ratio (CNR), i.e., VCF-STAP has the constant false alarm rate (CFAR) property with respect to CNR.

The new robust STAP detection statistic is constructed by the distance measure through the following steps.

First, the reciprocal of the VCF value is defined by

$$W(q) = 1/\mathrm{VCF}\left(\hat{\boldsymbol{T}}_s(q), \hat{\boldsymbol{T}}_t\right). \tag{9}$$

To form a peak value at the location of the target range cell for the new STAP detector, we compute the difference value $S^*(q)$ of $W(q)$ corresponding to the qth range cell, that is

$$S^*(q) = W(q) - W(q-1). \tag{10}$$

In this way, $S^*(q)$ has a large value when the energy of the target subspace is present at the qth range cell, i.e., the sample signal subspace intersects with the target subspace; otherwise, $S^*(q)$ tends to be a small value. However, the target energy leakage caused by pulse compression may result in the misalignment of the location of the target range cell for the detection in the STAP applications.

To eliminate the impact of the target energy leakage, a correction strategy is developed to correct the misalignment of the location of the target range cell. We use the correction area Θ to denote the set of range cells in which the target energy leakage exists. The correction area Θ is defined by

$$\Theta = \left\{q^*, q^*+1, \ldots, q^+-1, q^+\right\} \tag{11}$$

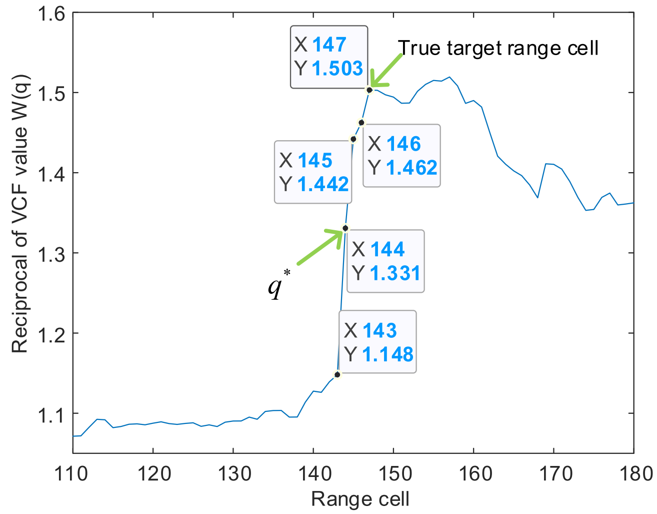

Fig. 1. Intuitive example to illustrate the construction of the detection statistic.

where $q^* = \max_q(S^*(q))$ is the first range cell of the correction area. The last range cell of Θ is the range cell that satisfies $S^*(q^+) \geq 0$ and $S^*(q^+ + 1) < 0$, i.e., starting from q^*, q^+ is the last range cell that satisfies $S^*(q^+) \geq 0$. Note that $W(q)$ is monotonically nondecreasing from q^* to q^+, i.e., $S^*(q) \geq 0$ when $q \in \Theta$.

Finally, the new detection statistic is constructed as

$$S(q) = \begin{cases} W(q) - W(q-1), q \notin \Theta \\ W(q) - W\left(q^* - 1\right), q \in \Theta \end{cases} \underset{H_0}{\overset{H_1}{\lessgtr}} \eta \tag{12}$$

where η is the detection threshold of VCF-STAP. Equation (12) can be explained in two aspects: 1) for the range cells that are not in the correction area, i.e., $q \notin \Theta$, the statistic is set to $S(q) = W(q) - W(q-1)$ and 2) for the range cells in the correction area, the statistic is corrected as $S(q) = W(q) - W(q^* - 1)$.

Next, we explain the effectiveness of (11). Due to the target energy leakage, the value of $W(q)$ increases gradually, i.e., there exists a rising edge in $W(q)$. Essentially, the correction area in (11) is the set of range cells corresponding to the rising edge of $W(q)$. By correcting the detection statistics corresponding to the range cells in (11), the new detection statistic $S(q)$ in (12) accumulates the leaked target energy and forms a peak value at the location of the target range cell.

An intuitive example to illustrate the construction of the detection statistic is shown in Fig. 1. Fig. 1 shows $W(q)$ in (9) versus the range cell based on the measured Mountain-Top data [10] by utilizing the spatial-temporal steering vector of the true target [11] with $Q = 40$. The starting range cell index q^* of Θ and the true target range cell are labeled in Fig. 1. It is verified that the true target is at the 147th range cell [11].

In Fig. 1, we show that $W(q)$ increases at 144–147th range cells, i.e., the area of the rising edge. The end of the rising edge is the 147th range cell. To form a peak value at the true target range cell, the statistics of the 144–147th range cells need to be corrected. It is consistent with the result of (11). By using the new detection statistic $S(q)$, VCF-STAP correctly detects the moving target by thresholding. The detection result will be shown in Fig. 4(a) in Section IV.

TABLE I

PARAMETERS OF SIMULATED AIRBORNE RADAR SYSTEM AND TARGET

Parameter	Quantity
Antenna array	Side-looking ULA
Antenna array spacing	Half-wavelength
Bandwidth	10MHz
Pulse repetition frequency	3000Hz
Platform velocity	150m/s
Platform height	10000m
Antenna elements number	14
Pulse number in one CPI	16
Normalized Doppler frequency of the target	0.08
Normalized spatial frequency of the target	0

Note that, by using (12), VCF-STAP not only generates a peak value at the target range cell, but also has the ability to distinguish targets with the spatial frequency and the Doppler frequency. Therefore, VCF-STAP has the ability to distinguish two targets even when their range cells are near to each other.

Different from existing distribution-based methods, the new VCF-STAP avoids the CCM estimation and the subsequent clutter suppression. It implements detection directly by determining whether the sample signal subspace and the target subspace intersect based on the VCF. VCF-STAP is a data-driven approach, which does not require any knowledge of the clutter distribution.

IV. EXPERIMENTAL RESULTS

In this section, the proposed VCF-STAP is compared with the distribution-based method, i.e., MAP [5], the traditional CCM estimation in STAP, i.e., sample covariance matrix (SCM) [12] based on the simulated data and measured Mountain-Top data. It should be noted that after the CCM estimation in the STAP technique by performing MAP and SCM, the adaptive matched filter [13] is exploited to implement the detection.

A. Simulation Results

In this section, the detection performance of VCF-STAP is evaluated with different approaches based on the simulated data. The parameters of the simulated radar and the inserted target are listed in Table I, and the averaged signal-to-clutter-plus-noise-ratio (SCNR) is formulated by Zhu *et al.* [14]

$$\text{SCNR} = \frac{\text{tr}\left[|\alpha|^2 \boldsymbol{s}\boldsymbol{s}^H\right]}{\frac{1}{Q}\sum_{q=1}^{Q} \text{tr}[\boldsymbol{R}(q)]} \tag{13}$$

where α is the complex target amplitude, $\boldsymbol{R}(q)$ denotes the CCM in the qth range cell, and $\text{tr}[\cdot]$ and $|\cdot|$ are the trace operator and the modulus operator, respectively.

The heterogeneous environment is considered here. Specifically, the CCM in the CUT is proportional to that in the training samples, and the maximum value of the scale factor is defined as the degree of heterogeneity ζ. In the simulations below, the number of training samples is set to $Q = 80$, which is much smaller than the degree of freedom of the radar system; the degree of heterogeneity is set to $\zeta = 40$. The prior covariance matrix employed in MAP is constructed as

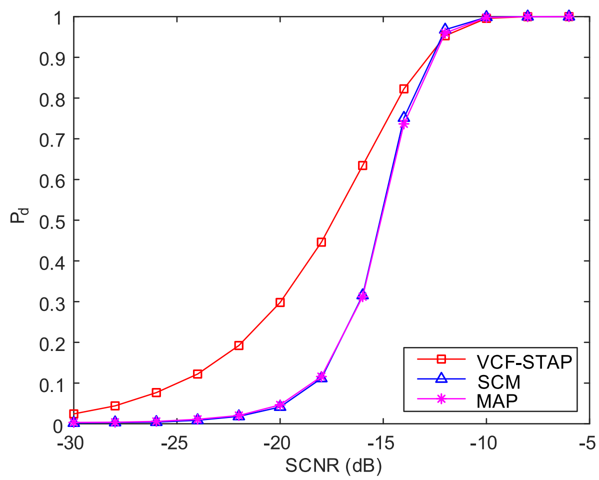

Fig. 2. P_{d} versus SCNR with $P_{\mathrm{fa}} = 10^{-3}$.

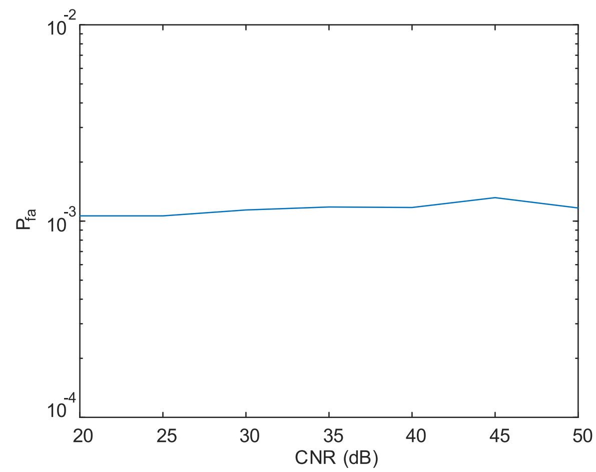

Fig. 3. P_{fa} versus CNR.

the perturbed version of the true clutter-and-noise covariance matrix according to the model in [14]. The degree of freedom of the assumed inverse Wishart distribution and that of the complex Wishart distribution in MAP are both empirically set to $2NM$. The threshold for each detector is determined from $100/P_{\mathrm{fa}}$ Monte Carlo simulations, where P_{fa} is the false alarm probability.

In Fig. 2, the detection probability P_{d} with respect to SCNR is illustrated with the parameter of $P_{\mathrm{fa}} = 10^{-3}$. Note that the low-speed target inserted in the simulated data is close to the clutter ridge in the angle-Doppler domain. In Fig. 2, we show that the detection probability of VCF-STAP is much higher than that of MAP and SCM when the SCNR is low. In other words, VCF-STAP achieves superior detection performance for moving targets to MAP and SCM in low SCNR cases, which always happen in STAP applications. The reason is that the VCF is sensitive to the energy of the target subspace, i.e., the detection statistic $S(q)$ would have a large value even if the target energy in the training sample matrix $\boldsymbol{X}(q)$ is low. Meanwhile, it should be noted that VCF-STAP implements detection by measuring the distance between the sample signal subspace and the target subspace without the requirement of modeling the clutter distribution. Therefore, VCF-STAP achieves robust detection performance in general heterogeneous environments even when the target is embedded in strong clutter environments.

The false alarm probability P_{fa} of VCF-STAP versus CNR is shown in Fig. 3. Because the columns of the basis matrices of $\mathcal{P}_s$ and $\mathcal{P}_t$ are normalized, the measurement of distance between $\mathcal{P}_s$ and $\mathcal{P}_t$ in (8) is independent of the clutter power. As a result, the threshold is independent of CNR. Therefore, VCF-STAP has the CFAR property with respect to CNR, as is clearly demonstrated in Fig. 3, consistent with our analysis in Section III-B. It proves again the superiority of VCF-STAP in target detection in heterogeneous environments.

In general, VCF-STAP yields the robust performance on target detection in heterogeneous environments. Especially, it achieves superior detection performance to distribution-based methods when clutter environments deviate from their prior assumption on the clutter distribution. Moreover, it is analyzed and validated that VCF-STAP has the CFAR property.

B. Experimental Results on Measured Data

In this section, the measured Mountain-Top data [10] are used to evaluate the performance of VCF-STAP. For the Mountain-Top data, the radar system is composed of 14 elements and 16 pulses in a CPI. It has been verified that the target in Mountain-Top data is at 147th range cell with a normalized Doppler frequency of 0.25 [11]. For SCM and MAP, the training data are selected around the CUT, excluding four guard cells. The prior covariance matrix used in MAP is designed according to the knowledge-aided covariance estimation [15] by utilizing the radar parameters [10]. The number of training samples is set to $Q = 40$ and other parameters are the same as the simulation part.

The range detection performances of the different approaches are demonstrated in Fig. 4. The maximum value of each curve is normalized to 1 and the normalized detection statistic of VCF-STAP is plotted on a [0,1] scale. Note that the detection performance is better when the values of the normalized detection statistics of the secondary range cells (i.e., the range cells except the target range cell) are lower.

It is shown in Fig. 4 that the normalized detection statistics of the secondary range cells of VCF-STAP are much lower than that of MAP and SCM; it demonstrates that VCF-STAP achieves the better detection performance than MAP and SCM based on measured data. The reason is that VCF-STAP implements detection without the prior assumption on the clutter distribution and, therefore, VCF-STAP yields a robust detection performance in real environments. Meanwhile, VCF-STAP corrects the misalignment of the location of the target range cell by employing the correction strategy, as depicted in Fig. 4(a). Thus, VCF-STAP is also robust to the target energy leakage. Besides, MAP yields unsatisfactory detection performance; the reason is that the real clutter environment does not match the assumed clutter distribution. SCM achieves poor detection performance due to the inaccurate estimation of the CCM by employing the insufficient number of IID training samples. In general, VCF-STAP can achieve robust performance of moving target detection in real clutter environments for STAP applications.

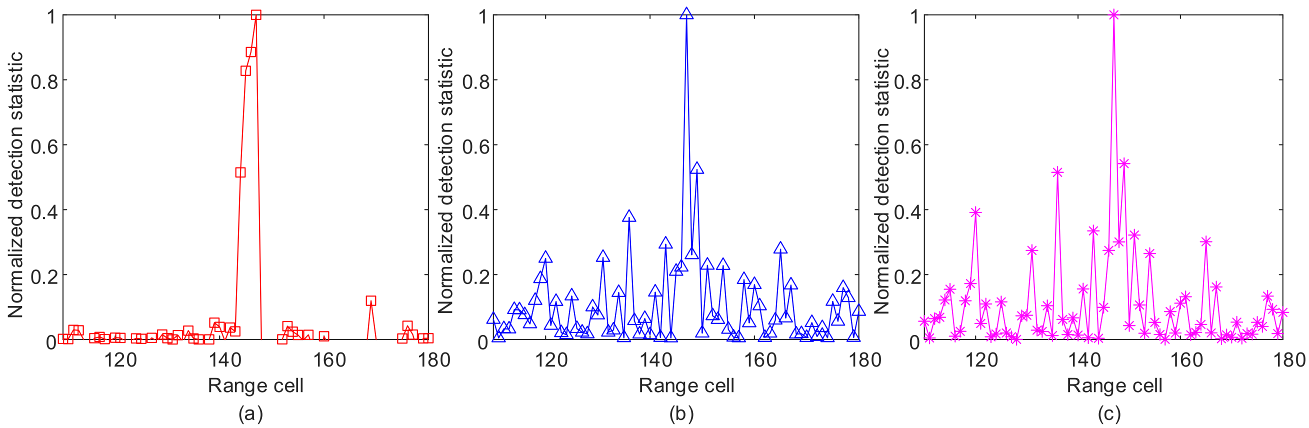

Fig. 4. Range detection performance of (a) VCF-STAP, (b) SCM, and (c) MAP based on measured Mountain-Top data.

V. Conclusion

In this letter, a new STAP detector based on VCF, namely VCF-STAP, is proposed to achieve robust moving target detection performance in heterogeneous environments. In the new VCF-STAP, the heterogeneous training samples are exploited to span the sample signal subspace, and the distance measure between the sample signal subspace and the target subspace is calculated by the VCF. Then, the new robust STAP detection statistic of VCF-STAP is formulated based on the difference value of the reciprocal of VCF values. A correction strategy is proposed to eliminate the misalignment of the location of the target range cell caused by the target energy leakage. Different from existing distribution-based methods, VCF-STAP avoids the CCM estimation and the clutter suppression. It implements detection directly by deciding whether the target subspace and the sample signal subspace intersect. VCF-STAP is a data-driven approach, which does not require any knowledge of the clutter distribution. Simulation and experimental results show that the new VCF-STAP outperforms existing methods such as MAP and SCM for moving target detection when the real clutter environments deviate from their assumed clutter distributions. Meanwhile, VCF-STAP is robust to the target energy leakage in the real scenario. More importantly, it is shown that VCF-STAP has the CFAR property. In general, VCF-STAP achieves robust detection performance in heterogeneous environments. Especially, it achieves superior detection performance to traditional distribution-based methods when the real clutter environments do not satisfy their prior assumption on the clutter distribution.

References

[1] Y. Wu, T. Wang, J. Wu, and J. Duan, "Training sample selection for space-time adaptive processing in heterogeneous environments," *IEEE Geosci. Remote Sens. Lett.*, vol. 12, no. 4, pp. 691–695, Apr. 2015.

[2] Z. Jiang, G. Li, X. Wang, X.-P. Zhang, and Y. He, "STAP based on two-level block sparsity," in *Proc. IEEE Radar Conf. (RadarConf)*, Boston, MA, USA, Apr. 2019, pp. 1–5.

[3] H. Yuan, H. Xu, K. Duan, W. Xie, and Y. Wang, "Cross-spectral metric smoothing-based GIP for space-time adaptive processing," *IEEE Geosci. Remote Sens. Lett.*, vol. 16, no. 9, pp. 1388–1392, Sep. 2019.

[4] Y. Wang, W. Liu, W. Xie, and Y. Zhao, "Reduced-rank space-time adaptive detection for airborne radar," *Sci. China Inf. Sci.*, vol. 57, no. 8, pp. 1–11, Aug. 2014.

[5] O. Besson, J.-Y. Tourneret, and S. Bidon, "Knowledge-aided Bayesian detection in heterogeneous environments," *IEEE Signal Process. Lett.*, vol. 14, no. 5, pp. 355–358, May 2007.

[6] O. Besson, S. Bidon, and J.-Y. Tourneret, "Covariance matrix estimation with heterogeneous samples," *IEEE Trans. Signal Process.*, vol. 56, no. 3, pp. 909–920, Mar. 2008.

[7] L. Xiao, H. Li, Y. Liu, and X. Wang, "Distributed target detection based on the volume cross-correlation function," *IEEE Signal Process. Lett.*, vol. 25, no. 12, pp. 1785–1789, Dec. 2018.

[8] H. Shi, H. Zhang, and X. Wang, "A TDOA technique with super-resolution based on the volume cross-correlation function," *IEEE Trans. Signal Process.*, vol. 64, no. 21, pp. 5682–5695, Nov. 2016.

[9] H. Shi, H. Zhang, and X. Wang, "A volume correlation subspace detector for signals buried in unknown clutter," in *Proc. IEEE Int. Symp. Inf. Theory (ISIT)*, Hong Kong, Jun. 2015, pp. 2196–2200.

[10] G. W. Titi and D. F. Marshall, "The ARPA/NAVY mountaintop program: Adaptive signal processing for airborne early warning radar," in *Proc. IEEE Int. Conf. Acoust., Speech, Signal Process. Conf.*, Atlanta, GA, USA, May 1996, pp. 1165–1168.

[11] S. Han, C. Fan, and X. Huang, "A novel STAP based on spectrum-aided reduced-dimension clutter sparse recovery," *IEEE Geosci. Remote Sens. Lett.*, vol. 14, no. 2, pp. 213–217, Feb. 2017.

[12] I. S. Reed, J. D. Mallett, and L. E. Brennan, "Rapid convergence rate in adaptive arrays," *IEEE Trans. Aerosp. Electron. Syst.*, vol. AES-10, no. 6, pp. 853–863, Nov. 1974.

[13] F. C. Robey, D. R. Fuhrmann, E. J. Kelly, and R. Nitzberg, "A CFAR adaptive matched filter detector," *IEEE Trans. Aerosp. Electron. Syst.*, vol. 28, no. 1, pp. 208–216, Jan. 1992.

[14] X. Zhu, J. Li, and P. Stoica, "Knowledge-aided space-time adaptive processing," *IEEE Trans. Aerosp. Electron. Syst.*, vol. 47, no. 2, pp. 1325–1336, Apr. 2011.

[15] S. Blunt, K. Gerlach, and M. Rangaswamy, "STAP using knowledge-aided covariance estimation and the FRACTA algorithm," *IEEE Trans. Aerosp. Electron. Syst.*, vol. 42, no. 3, pp. 1043–1057, Jul. 2006.